

ARTICLE TEMPLATE

A Supervised Abundance Estimation Method for Hyperspectral Unmixing

Xia Xu^{a,b,c}, Zhenwei Shi^{a,b,c} and Bin Pan^{a,b,c}

^aImage Processing Center, School of Astronautics, Beihang University, Beijing, China;
^bBeijing Key Laboratory of Digital Media, Beihang University, Beijing, China; ^cState Key Laboratory of Virtual Reality Technology and Systems, School of Astronautics, Beihang University, Beijing, China

ARTICLE HISTORY

Compiled December 1, 2017

ABSTRACT

Abundance estimation is one of the key steps in hyperspectral unmixing. Usually, abundance estimation is based on linear mixing. However, in real hyperspectral image, this assumption is not physically rigorous enough, because nonlinear mixture may be observed. Nonlinear models present an improvement by considering the microscopic interactions. However, in most cases, a nonlinear unmixing method should assume a specific nonlinear mixture model, and the corresponding abundance estimation process is only applicable for this model. Recently, supervised machine learning, especially deep learning methods, have achieved promising performance in hyperspectral image processing. Supervised learning is able to capture the mapping between input and output data. In this letter, a new supervised abundance estimation method is proposed, which aims to learn the mapping between pixels spectra and the fractional abundances. To overcome the difficulty that no groundtruth is available in real hyperspectral images, we propose a training samples generation strategy based on synthetic data. The major contribution of this work is that the proposed method can handle the abundance estimation problem in a uniform framework without assuming specific linear or nonlinear mixing model. Experiments on both synthetic and real data are conducted to validate the effectiveness of the proposed method.

KEYWORDS

Abundance estimation, hyperspectral unmixing, deep learning

1. Introduction

Hyperspectral images have the ability of covering hundreds of continuous spectral bands with abundant ground information. Recently, the research of hyperspectral remote sensing field is active and has attracted much attention. However, compared with the spectral resolution, the spatial resolution of hyperspectral images are relatively low. The earth surface region a pixel covers may include several materials. Hyperspectral unmixing is a technique aiming at separating the pixels into several elementary spectral signatures (endmembers) and their associated areal proportions (abundances). Generally, hyperspectral unmixing involves two steps: endmembers determination and abundances estimation. However, due to the problems such as model inaccuracies and

ill-posed abundance inversion, hyperspectral unmixing is still challenging (Keshava and Mustard 2002).

Hyperspectral unmixing relies on the predesigned mixing model which can be described either linearly or nonlinearly. Linear mixing model (LMM), which neglects the effects of multiple scattering and intimate mixture, is the most prevalent (Bioucas-Dias et al. 2012). A number of efforts have been devoted to solving the linear unmixing problem, including geometry, statistics, nonnegative matrix factorization and sparse based unmixing (Bioucas-Dias et al. 2012; Xu and Shi 2017). However, LMM is not a rigorous expression of hyperspectral image in many real scenarios, such as intimate mineral mixtures, planetary remote sensing and some urban scenes (Heylen, Parente, and Gader 2014). Physically, the nonlinear components, i.e., microscopic interactions among endmembers, should also be taken into account. Recently, many researchers attempted to represent the nonlinearity as an extra component of LMM, such as the Fan model (Fan et al. 2009), generalized bilinear model (GBM) (Halimi et al. 2011), modified GBM (MGBM) (Qu, Nasrabadi, and Tran 2014), polynomial postnonlinear model (PPNMM) (Altmann et al. 2012) and multilinear mixing model (MLM) (Heylen and Scheunders 2016). However, for abundance estimation, most nonlinear unmixing algorithms are model-dependent, i.e., an unmixing method is only applicable for a certain nonlinear model assumption (Heylen, Parente, and Gader 2014). If the assumed model does not exactly match the real situation, the unmixing results cannot be guaranteed. Unfortunately, in real-world hyperspectral images, it is almost impossible to obtain the prior mixing model of different image. Moreover, the commonly used nonnegative least square algorithm (NNLS) may not perform well for most nonlinear models.

In order to solve the above problem, in this letter, we propose a new supervised abundance estimation method. Supervised machine learning, especially deep learning methods, have achieved promising performance in hyperspectral remote sensing, e.g., hyperspectral image classification (Pan, Shi, and Xu 2017). Supervised learning aims at representing the mapping between input and output data via a data-driven manner. Recently, deep learning, which could be regarded as an extension of traditional machine learning, has received special attention. In Cybenko (1989), Cybenko proposed the Universal Approximation Theorem, revealing that the multi-layer perception model can approximate any continuous function with any precision as long as enough neurons are given. Motivated by the powerful expression ability of supervised learning, in this letter, we develop a new supervised approach to deal with the problem of abundance estimation via learning the mapping relationship between pixels spectra and the abundance fractions. In addition, considering that it is almost impossible to obtain labeled pixels from real-world hyperspectral data, we try to create training samples based on synthetic data.

The major contributions of this work can be summarized as follows,

- We propose a novel supervised method which could handle the abundance estimation problem in a uniform framework without assuming specific linear or nonlinear mixture model.
- A training samples generation strategy is developed based on synthetic data and diverse mixture models.
- We explore the feasibility of deep learning methods in hyperspectral unmixing, and a series of experiments are designed.

Experiments on synthetic and real data are conducted to verify the effectiveness of the proposed method, and the results indicate that deep learning methods are promising for the task of hyperspectral unmixing. Specially, we find that even the

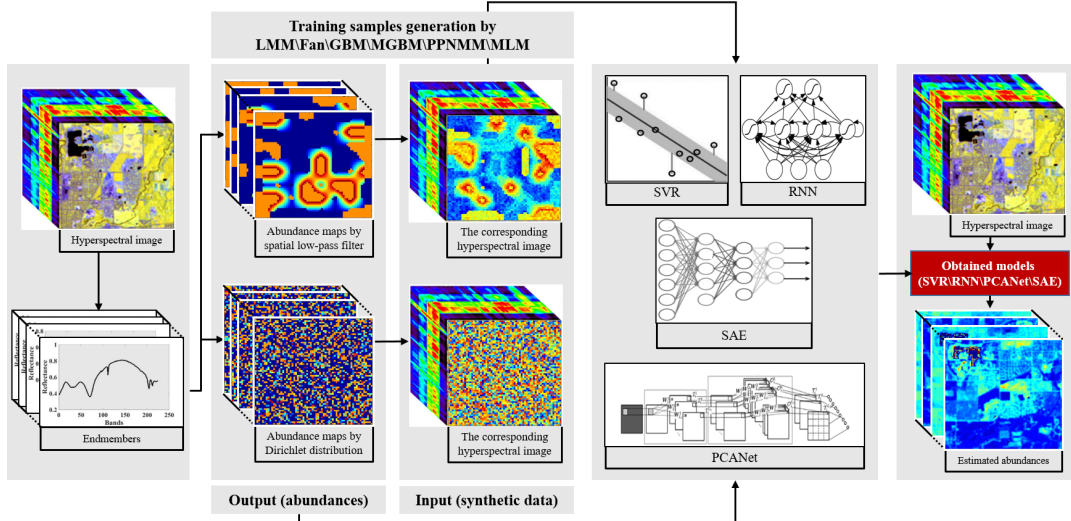


Figure 1.: Illustration of the overall framework of the proposed supervised unmixing method.

mixing manner of testing data is not embedded in training data, the proposed method still performs well.

2. Supervised hyperspectral unmixing

NNLS is commonly used in abundance inversion for LMM-based unmixing, whereas it is not appropriate in nonlinear conditions. Usually, for a nonlinear model, there must be a specific abundance estimation algorithm. Based on supervised learning, the proposed abundance estimation method overcomes the limitation and does not require strict linear or nonlinear model. Since the unmixing groundtruth of hyperspectral image is difficult to obtain, we propose a training samples generation strategy. LMM as well as five published nonlinear models are used to create training samples, namely, LMM, Fan, GBM, MGBM, PPNMM, MLM. These models stem from the physical analysis of hyperspectral imaging mechanism, which are representative in this field. Based on the obtained training samples and the corresponding label, we use four kinds of regression methods to estimate the abundances of testing data, namely, support vector regression (SVR) (Smola and Schölkopf 2004), recurrent neural network (RNN) (Elman 1990), principal component analysis network (PCANet) (Chan et al. 2015) and stacked autoencoder (SAE) (Palm 2012). The overall framework of the proposed supervised unmixing method is illustrated in Fig. 1. And the procedure is shown in Algorithm 1.

2.1. Training samples generation

Because hyperspectral unmixing is a subpixel-based problem, it is difficult to obtain an effective groundtruth. In this letter, we propose a training sample generation method based on synthetic data. Since we mainly focus on the process of abundance estimation, here, we assume that the endmembers have been obtained by endmember extraction methods such as vertex component analysis (VCA) (Nascimento and Dias

Algorithm 1 Procedure of the proposed method

Input:

\mathbf{Y} : hyperspectral image data; \mathbf{e}_i : spectra of endmembers.

Training samples generation:

- 1: **for** endmember \mathbf{e}_i **do**
- 2: Create an abundance map based on spatial low-pass filter or Dirichlet distribution.
- 3: **end for**
- 4: Generate a hyperspectral image according to LMM, Fan, GBM, MGBM, PPNMM, MLM.

Supervised abundance estimation:

- 5: Use the synthetic data and abundance maps to train the SVR, RNN, PCANet, SAE respectively.
- 6: Estimate the abundance map of \mathbf{Y} based on the four methods.

Output:

- 7: The abundance map of \mathbf{Y} .
-

2005). Abundances of the synthetic samples are generated by spatial low-pass filter and Dirichlet distribution. Then synthetic training data are created based on the six well-known linear and nonlinear models. Specially, all the pure pixels are removed. The detail description of the data generation method is shown in the experimental section. It is worth mentioning that any number of samples can be generated based on different methods.

Theoretically, in order to make the regression methods be able to handle any nonlinearity, it is necessary to generate training data by all nonlinear models. However, the spectral mixture model is unknown in reality. In addition, the mixture models in different hyperspectral data is likely to be diverse. Therefore, it is impossible to generate the training data that exactly match all real cases. In this letter, we use the existing nonlinear models as many as possible to better approximate the actual mixture. The six well-known linear and nonlinear models are introduced as follows.

2.1.1. Linear model

For LMM, each pixel can be approximated as a linear combination of several pure spectral signatures in a spectral library (Keshava and Mustard 2002):

$$\mathbf{y} = \sum_{i=1}^m a_i \mathbf{e}_i + \mathbf{n} \quad (1)$$

where $\mathbf{y} \in \mathbb{R}^{l \times 1}$ is the measured spectrum of a mixed pixel, $\mathbf{e}_i \in \mathbb{R}^{l \times 1}$ denotes the i th spectral signature (m is the number of endmembers), a_i is the abundance of the i th endmember, and \mathbf{n} is the noise and modeling error term.

2.1.2. Fan model

Fan model is derived from the Taylor series expansions of the assumed nonlinear function and simplified by only reserving the first-order item. It considers the interaction among two different materials (Fan et al. 2009):

$$\mathbf{y} = \sum_{i=1}^m a_i \mathbf{e}_i + \sum_{i=1}^{m-1} \sum_{j=i+1}^m a_i a_j \mathbf{e}_i \odot \mathbf{e}_j + \mathbf{n} \quad (2)$$

where $\mathbf{e}_i \odot \mathbf{e}_j$ is the Hadamard (term-by-term) product.

2.1.3. Generalized bilinear model

GBM is an extension of Fan model. The interaction between two endmembers is regulated by introducing an additional coefficient γ_{ij} (Halimi et al. 2011):

$$\mathbf{y} = \sum_{i=1}^m a_i \mathbf{e}_i + \sum_{i=1}^{m-1} \sum_{j=i+1}^m \gamma_{ij} a_i a_j \mathbf{e}_i \odot \mathbf{e}_j + \mathbf{n} \quad (3)$$

2.1.4. Modified GBM

MGBM improves GBM by adding endmembers' self-product and also considers the effects of materials from nearby pixels (Qu, Nasrabadi, and Tran 2014):

$$\mathbf{y} = \sum_{i=1}^m a_i \mathbf{e}_i + \sum_{i=1}^m \sum_{j=i}^m \gamma_{ij} a_i a_j \mathbf{e}_i \odot \mathbf{e}_j + \mathbf{n} \quad (4)$$

2.1.5. Polynomial postnonlinear model

PPNMM is inspired by the Weierstrass approximation theorem, which indicates that polynomials can uniformly approximate any bounded continuous function with any precision. It models the nonlinearity mixing as (Altmann et al. 2012):

$$\mathbf{y} = \sum_{i=1}^m a_i \mathbf{e}_i + b \left(\sum_{i=1}^m a_i \mathbf{e}_i \right) \odot \left(\sum_{i=1}^m a_i \mathbf{e}_i \right) + \mathbf{n} \quad (5)$$

where b scales the nonlinear effects and makes PPNMM flexible.

2.1.6. Multilinear mixing model

MLM extents PPNMM to include all higher order interactions, which makes nonlinear models more physically. In this case, the nonlinear model is defined by (Heylen and Scheunders 2016):

$$\mathbf{y} = \sum_{i=1}^m a_i \mathbf{e}_i + \left(\sum_{i=1}^m a_i \mathbf{e}_i \right) \odot \left(\sum_{i=1}^m a_i \mathbf{e}_i \right) + \dots \quad (6)$$

However, our method does not restrict to the hyperspectral data that complies with these six models. In fact, the proposed method has good expandability. The main reason is that the relationship between different models can also be learned by the regression methods. This conclusion is verified in the experimental section.

2.2. Supervised abundance estimation

In this letter, supervised regression methods are used to learn the mapping between image data and abundances. The basic idea of the proposed method is that machine learning, especially deep learning, can learn the complex relationship between input and output data. Then abundance estimation can be effectively performed by the regression methods. In this letter, the following four methods are utilized for abundance

estimation: SVR, RNN, PCANet and SAE. Among them, SVR is a traditional machine learning method, which can be used as a baseline. RNN is a neural network based regression forecasting method, and has made great achievements in language processing. PCANet and SAE are deep learning based methods, which have becoming one of the most hot topics in computer vision. PCANet is a simplified version of convolution-based deep learning network, and has been applied in hyperspectral image classification (Chan et al. 2015). SAE is a deep learning network that can extract deep features of hyperspectral images.

First, we generate a group of synthetic data based on the above 6 mixing models. The synthetic data are composed of many mixed pixels and the corresponding abundance maps. Second, we consider each pixel and the endmember abundance as a feature vector and the label, respectively. Then, all the features and labels are used to train a regression model (SVR, RNN, PCANet or SAE). Finally, the obtained model is utilized to estimate the endmember abundances in real-world hyperspectral images. Since the synthetic data are generated by various mixing models, the proposed method does not need to assume a particular mixing model.

3. Experiments

A series of synthetic and real-world experiments are designed in this section. Synthetic data are generated by five materials and six mixing models (LMM, Fan, GBM, MGBM, PPNMM and MLM). The number of training samples are shown in Table 1. SVR, RNN, PCANet and SAE are used to verify the proposed method respectively. Radial Basis Function kernel is used in SVR. Parameters of these networks are adjusted according to unmixing problem. The proposed method is actually a framework for abundance estimation, therefore the parameters analysis is not included in this letter. The Matlab code of this letter is published online¹.

3.1. Synthetic experiments

The spectral signatures used in synthetic data are from the USGS spectral library released in 2007². Five similar spectral signatures named Actinolite HS116.3B, Actinolite HS22.3B, Actinolite HS315.4B, Actinolite NMNH80714 and Actinolite NMNHR16485, are selected specially to generate the synthetic data. All the synthetic data are created as follows.

- Create a $z^2 \times z^2$ scene and block it into several $z \times z$ patches. Each patch is initialized pure of a randomly selected signature.
- Generate abundances based on a $(z+1) \times (z+1)$ spatial low-pass filter or Dirichlet distribution.
- Find all the pixels in which an endmember occupies larger than 70% abundance, and replace them by random variety of endmembers and fraction combinations. The replacement is to avoid pure pixels and better test the proposed method.
- Use the LMM, Fan, GBM, MGBM, PPNMM and MLM to generate hyperspectral data. It is worth to note that MGBM and PPNMM have the same parameter setting for experiment, so we only use PPNMM for representative.

¹Available online: <http://levir.buaa.edu.cn/>

²Available online: <http://speclab.cr.usgs.gov/spectral.lib06>

Table 1.: The SRE results of SVR, RNN, PCANet and SAE with 30-dB correlated noise. The number of training samples for different regression models is presented in brackets.

training data	testing data	SVR (50)	RNN (100)	PCANet (100)	SAE (2000)	NNLS	GBM
LMM, Fan, GBM, PPNMM, MLM	LMM	12.98	9.49	8.40	14.49	14.34	15.94
	Fan	13.37	9.36	8.28	14.35	6.65	3.72
	GBM	13.46	9.86	8.81	14.53	10.68	11.87
	PPNMM	12.57	9.53	8.08	13.45	10.48	6.47
	MLM	12.35	9.14	8.55	13.61	12.61	9.58

Table 2.: The SRE results of SAE on different noise levels, noise types and abundance generation mode. ‘20c’ and ‘20w’ denote 20-dB correlated and white noise respectively.

	20c	20w	30c	30w	40c	40w
Low-pass filter	7.11	7.11	14.19	14.19	18.05	18.14
Dirichlet distribution	7.20	7.07	14.61	14.61	18.74	18.78

The synthetic experiments are divided into two groups.

3.1.1. Evaluation on Synthetic Data 1

Synthetic data 1 are generated by all the linear and nonlinear models and randomly sorted as training samples. White and correlated noises with different signal-to-noise ratios ($\text{SNR} = 10\log_{10}(\|\mathbf{Y}\|_{\text{F}}^2/\|\mathbf{N}\|_{\text{F}}^2)$) are added to the testing data respectively. For each regression method, we test its performance on five data types created by LMM, Fan, GBM, PPNMM and MLM respectively. The testing data are certainly regenerated. We also evaluate the proposed method with a popular linear unmixing method, NNLS, as well as a nonlinear method, GBM, as shown in Table 1. Table 1 is the signal to reconstruction error (SRE) ($\text{SRE} = 10\log_{10}(\mathbf{E}[\|\mathbf{X}\|_{\text{F}}^2]/\mathbf{E}[\|\mathbf{X} - \hat{\mathbf{X}}\|_{\text{F}}^2])$) results of SVR, RNN, PCANet and SAE with 30-dB correlated noise. SVR, RNN and PCANet are traditional classifiers or shallow neural networks, so 50-100 samples are enough for training. SAE is a deep learning model, thus we use 2000 samples for training. According to the results, GBM performs best in LMM, and SAE present similar performance as NNLS. However, the major advantage of the proposed method is that we do not need to design specific algorithm to handle different models. The testing results of different data type have small fluctuation. This is reasonable since the training samples can cover all the five data types. It can also be observed that SAE performs the best among all the four regression methods. Therefore, the SAE results on different noise level, different noise type, and different abundance generation mode are presented in Table 2 to test their effect. The testing data is generated based on MLM in this case. From Table 2, the results become better for weaker noise, and are not sensitive to the noise type and the generation mode of abundance.

Table 3.: The SRE results on Synthetic Data 2 with 20-dB, 30-dB and 40-dB correlated noise.

training data	testing data	20c	30c	40c
LMM, Fan, GBM, PPNMM	MLM	6.78	14.02	15.76
LMM, Fan, GBM	MLM	7.64	13.66	16.02
LMM, Fan, GBM, MLM	PPNMM	6.78	13.32	15.04
LMM, MLM	PPNMM	6.85	8.65	9.95
Fan, GBM, PPNMM, MLM	LMM	6.81	14.38	16.81

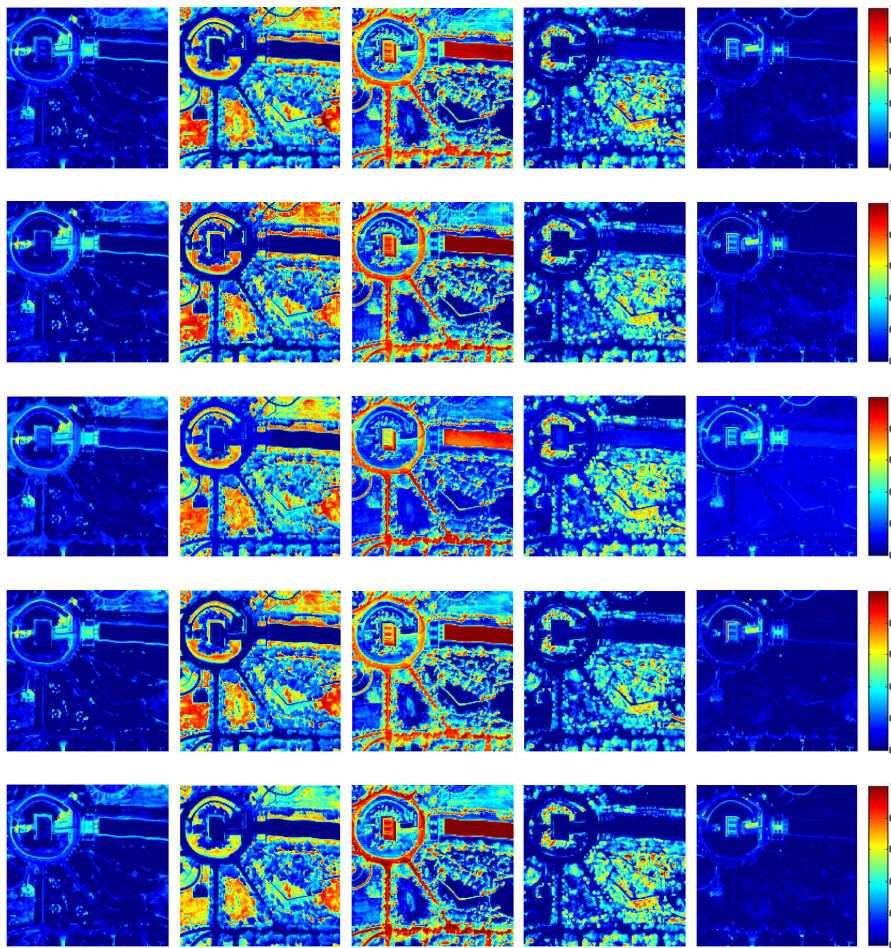


Figure 2.: Abundance maps obtained by the four regression methods. From top to the bottom are abundance maps of the five materials obtained by SVR, RNN, PCANet, SAE, NNLS, respectively.

3.1.2. Evaluation on Synthetic Data 2

We designed the second synthetic experiment, where testing data are obtained by none of the mixing models in training data. In this experiment, training and testing data are generated based on different mixing models, as shown in Table 3. Here we only report the results by SAE, because SAE performs better than other methods according to Table 1. Comparing the results in Table 1 and Table 3, we note that the gaps are little in 30-dB noise. Furthermore, it is observed that, for a given testing model, more training models will bring better results, as shown in lines 2 and 3, line 4 and 5 at Table 3. This experiment indicates that by utilizing mixing models as many as possible for training, the abundance estimation results are satisfying, even though the real mixing model is not included in training data.

3.2. Real-world experiments

A real-world data is also used to test the performance of the proposed method. The hyperspectral data we use is a 150×150 subset from the well-known Washington DC data³, which has 191 bands after low-SNR bands removed. It is known that the image mainly contains five cover types, including tree, grass, road, roof and water. Because the groundtruth of real-world data is not available, we resort to the synthetic data to generate training samples and make a qualitative analysis in this case. The training data are generated synthetically by the above five models. In order to verify the performance of the proposed method, we take the results of NNLS as comparison for SVR, RNN, PCANet and SAE. The abundance maps of the five materials are shown in Fig. 2. We can see that all the five methods have shown similar performance. In endmember 2, the four regression methods perform better than NNLS. Experiments on this real world dataset could verify that the proposed method is effective. At least, the idea of the new supervised unmixing is promising.

4. Conclusion

Abundance estimation is one of the key steps in hyperspectral unmixing. Although the LMM assumption is prevalent for unmixing methods, it is not rigorous in real-world cases. Nonlinear model makes up for this problem by considering more physical mechanism in imaging process. However, the corresponding nonlinear unmixing method is usually model-dependant. In this letter, a supervised abundance estimation method is proposed. This method can avoid the use of strict linear or nonlinear models and the functional inversion in abundance estimation. Considering the lack of groundtruth of hyperspectral unmixing, training samples are generated based on synthetic data. For the generating process, we resort to the recently presented linear and nonlinear models. Furthermore, machine learning especially deep learning are used to model the relationship between the image data and abundance fractions. Our experiments on both synthetic and real hyperspectral data demonstrate the good performance of the proposed method. The proposed work is actually a framework for abundance estimation, and it is easy to improve the performance by using more representative learners. Our future work will be designing a more powerful deep learning based network to achieve better abundance estimation performance.

³Available online: <https://engineering.purdue.edu/biehl/MultiSpec>

5. Acknowledgement

This work was supported by the National Natural Science Foundation of China under the Grants 61671037, the Beijing Natural Science Foundation under the Grant 4152031, and the Excellence Foundation of BUAA for PhD Students under Grant 2017057.

References

- Altmann, Yoann, Abderrahim Halimi, Nicolas Dobigeon, and Jean-Yves Tourneret. 2012. “Supervised nonlinear spectral unmixing using a postnonlinear mixing model for hyperspectral imagery.” *IEEE Transactions on Image Processing* 21 (6): 3017–3025.
- Bioucas-Dias, José M, Antonio Plaza, Nicolas Dobigeon, Mario Parente, Qian Du, Paul Gader, and Jocelyn Chanussot. 2012. “Hyperspectral unmixing overview: Geometrical, statistical, and sparse regression-based approaches.” *IEEE Journal of Selected Topics in Applied Earth Observations and Remote Sensing* 5 (2): 354–379.
- Chan, Tsung-Han, Kui Jia, Shenghua Gao, Jiwen Lu, Zinan Zeng, and Yi Ma. 2015. “PCANet: A simple deep learning baseline for image classification?” *IEEE Transactions on Image Processing* 24 (12): 5017–5032.
- Cybenko, George. 1989. “Approximation by superpositions of a sigmoidal function.” *Mathematics of control, signals and systems* 2 (4): 303–314.
- Elman, Jeffrey L. 1990. “Finding structure in time.” *Cognitive science* 14 (2): 179–211.
- Fan, Wenyi, Baoxin Hu, John Miller, and Mingze Li. 2009. “Comparative study between a new nonlinear model and common linear model for analysing laboratory simulated-forest hyperspectral data.” *International Journal of Remote Sensing* 30 (11): 2951–2962.
- Halimi, Abderrahim, Yoann Altmann, Nicolas Dobigeon, and Jean-Yves Tourneret. 2011. “Nonlinear unmixing of hyperspectral images using a generalized bilinear model.” *IEEE Transactions on Geoscience and Remote Sensing* 49 (11): 4153–4162.
- Heylen, Rob, Mario Parente, and Paul Gader. 2014. “A review of nonlinear hyperspectral unmixing methods.” *IEEE Journal of Selected Topics in Applied Earth Observations and Remote Sensing* 7 (6): 1844–1868.
- Heylen, Rob, and Paul Scheunders. 2016. “A multilinear mixing model for nonlinear spectral unmixing.” *IEEE Transactions on Geoscience and Remote Sensing* 54 (1): 240–251.
- Keshava, Nirmal, and John F Mustard. 2002. “Spectral unmixing.” *IEEE Signal Processing Magazine* 19 (1): 44–57.
- Nascimento, José MP, and José MB Dias. 2005. “Vertex component analysis: A fast algorithm to unmix hyperspectral data.” *IEEE transactions on Geoscience and Remote Sensing* 43 (4): 898–910.
- Palm, Rasmus Berg. 2012. “Prediction as a candidate for learning deep hierarchical models of data.” *Technical University of Denmark* 5.
- Pan, B., Z. Shi, and X. Xu. 2017. “R-VCANet: A New Deep-Learning-Based Hyperspectral Image Classification Method.” *IEEE Journal of Selected Topics in Applied Earth Observations and Remote Sensing* 10 (5): 1975–1986.
- Qu, Qing, Nasser M Nasrabadi, and Trac D Tran. 2014. “Abundance estimation for bilinear mixture models via joint sparse and low-rank representation.” *IEEE Transactions on Geoscience and Remote Sensing* 52 (7): 4404–4423.
- Smola, Alex J, and Bernhard Schölkopf. 2004. “A tutorial on support vector regression.” *Statistics and computing* 14 (3): 199–222.
- Xu, Xia, and Zhenwei Shi. 2017. “Multi-objective based spectral unmixing for hyperspectral images.” *ISPRS Journal of Photogrammetry and Remote Sensing* 124: 54–69.